

Improved Blade Element Momentum theory (BEM) for Predicting the Aerodynamic Performances of Horizontal Axis Wind Turbine Blade (HAWT)

Y. El khchine, M. Sriti

In this work, a mathematical model based on the compact Blade Element Momentum theory (BEM) is used to design a horizontal axis wind turbine blade. This implemented method is applied to evaluate the aerodynamic performance of a wind turbine blade and gives new optimized blade geometry. The rated power, free stream wind speed, design tip speed ratio, number of blades and optimal angle of attack are considered as design parameters. To validate the new approach, the results of the modified BEM presented in this work are analyzed and compared with previous works presented in the literature.

1 Introduction

Wind turbine blade design plays a critical role in producing maximum power studied among others by (Hassanzadeh et al., 2016). There have been different computational tools to design wind turbine blades. Computational Fluid Dynamic (CFD) is widely used as a design tool, which produces accurate results. On the other hand, longer time for calculation and big informatics memory is needed (El khchine and Sriti, 2017). The mathematical model based on Blade Element Momentum theory (BEM) is most frequently used in industry and scientific research due to its mid-fidelity results but with less time expenses. The BEM provides the capability to determine the optimal rotor geometry with maximum power design and to evaluate the forces and torque acting on the blades. The optimal design of blade geometry is based on several parameters: rotor angular speed, number of blades, length of blades, twist angle. In wind turbine aerodynamics, it was reported by many researchers that the Blade Element Momentum method (BEM) (Glauert, 1935; Manwell and McGowan, 2010) is the most widely used as an acceptably efficient approach for wind turbine blade design and analysis (Singh et al., 2012). (Maalawi et al., 2003) presented an approach to obtain the optimal relative angle of wind for a given rotor diameter and rotor solidity. (Vitale, 2008) developed a code to obtain the optimum blade shape for HAWT with optimum rotor power efficiency. The heuristic process of blade design based on the Blade Element Momentum theory was accelerated by involving advanced optimization strategies, such as evolutionary algorithms (Benini, 2002). These methods showed advanced computing efficiency as well as a reduced work load and allow a rapid blade design. In the design of small blades, a high number of influences has to be considered because the small wind turbines experience much lower Reynolds number flow than the large wind turbines, and the hub and tip area is vital for the starting-up torque which should be able to conquer the resistance of the system.

However, some assumptions in the BEM equations lead to discrepancies between experimental data and BEM results. One of the assumptions contains the negligence of the static pressure drop caused by wake rotation such that the pressure in far upstream of the rotor equals the condition in far downstream. Based on this assumption, it is derived that the axial induction at the rotor disc is half of that in the far wake. (Joukowsky, 1912) considered the effect of wake rotation in the analysis of propellers, which leads to the increase in rotor power coefficient at low tip speed ratio. (Wilson and Lissaman, 1974) adopted wake rotation in the analysis of wind turbine. The

axial induction factor at the disc is always smaller than half of that in infinitely far downstream at tip speed ratio below 2. (Vries, 1979) made a similar analytical study on the consequences of non-rotating wake but he did not apply this to the BEM theory and disregarded the additional pressure change caused by wake rotation. (Sharpe, 2004) reiterated the full analysis of the general momentum theory. He came to the conclusion that the rotor power coefficient increases at low tip speed ratio and can exceed the Betz-Joukowsky limit. The equations forming the general momentum theory of wind turbine rotors were clearly analyzed by (Sørensen et al., 2011) where they derived a most general momentum theory which can be used to get the known momentum theories such as the Glauert model or the Burton model. However, the assumption of ignoring radial velocity in the general momentum theory also needs to be improved. According to the MEXICO experiment by (Schepers et al., 2012), a significant radial flow can be seen at places just before the rotor blade. The influences of the radial flow have not been considered in both classic momentum theory and general momentum theory. (Lanzafame and Messina, 2012) described mathematically the lift coefficients to eliminate the lack of description for centrifugal pumping and the results have been compared with experimental data in scientific literature for the power and efficiency curves of NREL phase VI turbine. The constant and varied rotational velocity effects on mechanical power were studied and compared (Lanzafame and Messina, 2010). (Kim et al., 2013), have developed the software BOT (Blade Optimization Tool) for designing the optimum shape of multi-MW wind turbine blades and analyzed its performance, to verify the accuracy of their research. The results were compared with the results obtained by commercial software GH-Bladed.

This work presents a modified Blade Element Momentum theory (BEM) to predict the aerodynamic performances of NREL Phase VI. A new formulation of axial induction factor was introduced in this work by applying a new approximation of loss factor to correct the wake phenomenon. As a result, this model can give optimal blade geometry (change of chord length, twist angle and power coefficient).

2 Mathematical Modeling

The Blade Element Momentum theory can be subdivided into two parts. In the first part, the blade is divided into several independent elements. Further, it is assumed that the aerodynamic forces on each element can be calculated as a two-dimensional airfoil subjected to the flow conditions. Figures (1) and (2) show a cross section of a rotor blade. Velocities and forces related to the blade are shown in these cross sections of the rotor blade.

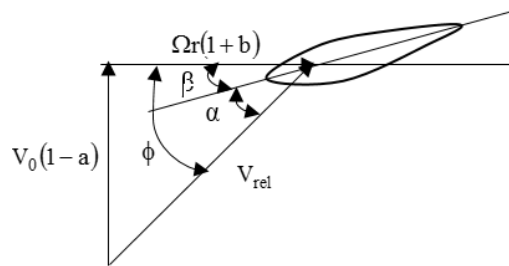


Figure 1. Cross sectional airfoil element

a and b are the axial and angular induction factors respectively. V_0 is the free stream wind velocity, Ω is the angular velocity of rotor.

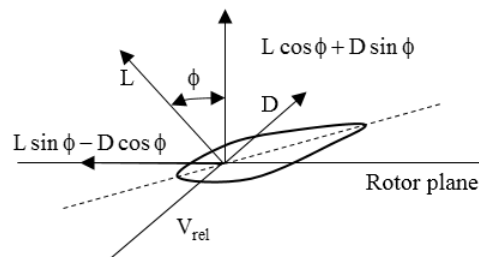


Figure 2. Blade element forces

Furthermore, the lift and drag forces L and D respectively are defined as

$$L = \frac{1}{2} \rho V_0^2 A C_l \quad (1)$$

$$D = \frac{1}{2} \rho V_0^2 A C_d \quad (2)$$

with the rotor area A and the lift and drag coefficients C_l and C_d respectively.

In Figure 1, ϕ is the angle of relative wind to the rotor plane which is the sum of section pitch angle, β , and angle of attack, α . The section pitch angle is equal to pitch angle along the blade in untwisted blades and varies locally in twisted blades. It mainly depends on the blade control system, blade geometry and elastic deflection. The angle of attack is mainly dependent on the element radial speed, upstream wind velocity, and induced velocity. Figure 2 shows the aerodynamic forces on the blade and their components perpendicular and parallel to the rotor plane with the rotor radius R , the local radius r and the chord length c .

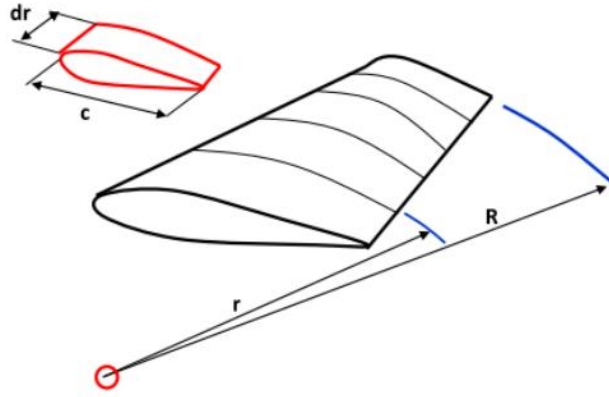


Figure 3. Blade element model

The perpendicular component is the main element to the rotor thrust; while the parallel component is responsible for the rotor torque. The blade is divided into several elements as shown in Figure 3, by applying the equations of mass and angular momentum conservation for each element dr , thrust and torque for a system with B blades can be defined by equations (3) and (4), respectively

$$dT = \frac{1}{2} \rho B V_0^2 \frac{(1-a)^2}{\sin^2 \phi} c (C_l \cos \phi + C_d \sin \phi) dr \quad (3)$$

$$dM = \frac{1}{2} \rho B V_0 \frac{(1-a)(1+b)}{\sin \phi \cos \phi} c (C_l \cos \phi - C_d \sin \phi) r dr . \quad (4)$$

The second part in the Blade Element Momentum theory is to apply the conservation of momentum. According to the momentum theory, the net force on the actuator disk comes from the change of air momentum passing through the disk; and the rate of momentum is equivalent to the air velocity difference across the rotor plane times the mass flow rate. Hence, the thrust and torque can be written as

$$dT = 4\pi \rho B V_0^2 a(1-a)r dr \quad (5)$$

$$dM = 4\pi \rho B V_0 \Omega b(1-a)r^3 dr . \quad (6)$$

Now, if one substitutes the left sides of equations (5) and (6) with the right sides of equations (3) and (4), respectively, the factors of the induced velocity can be obtained as

$$a = \frac{\sigma C_n}{4 \sin^2 \phi + \sigma C_n} \quad (7)$$

$$b = \frac{\sigma C_t}{4 \sin \phi \cos \phi - \sigma C_t} \quad (8)$$

with the normal and tangential loads coefficients C_n and C_t respectively

$$\begin{aligned} C_n &= C_l \cos \phi + C_d \sin \phi \\ C_t &= C_l \sin \phi - C_d \cos \phi \end{aligned} \quad (9)$$

where σ is the solidity of rotor defined as

$$\sigma = \frac{Bc}{2\pi r} .$$

The inflow angle ϕ is determined by

$$\tan \phi = \frac{V_0(1-a)}{\Omega r(1+b)} . \quad (10)$$

2.1 Prandtl's Loss Factor Correction

Before solving the above system of equations, which is the original Blade Element Momentum theory, some corrections can be made. One of the limitations of the original BEM theory is that the effects of vortices shedding by the blade tip to the wake are neglected, despite the fact that these vortices play a significant role in the induced velocity distribution at the rotor. The second limitation states that the above equations are only valid for rotors with infinite many blades. (Prandtl, 1927) was the first to address this issue. According to the Prandtl theory, in order to incorporate the tip loss in the original BEM equation, one may change equations (5) and (6) as follows

$$dT = 4\pi\rho BV_0^2 a(1-a)Frdr \quad (11)$$

$$dM = 4\pi\rho BV_0\Omega b(1-a)Fr^3 dr \quad (12)$$

where F is the tip-hub loss factor, which is obtained as

$$F = \begin{cases} F_{hub} & \text{if } r \leq 0.8R \\ F_{tip} & \text{if } r > 0.8R \end{cases} \quad (13)$$

with

$$\begin{aligned} F_{tip} &= \frac{2}{\pi} \cos^{-1} \left(\exp \left(-\frac{B(R-r)}{2r \sin \phi} \right) \right) \\ F_{hub} &= \frac{2}{\pi} \cos^{-1} \left(\exp \left(-\frac{B(r-r_{hub})}{2r \sin \phi} \right) \right) . \end{aligned}$$

Therefore, the new form of equations (7) and (8) can be written as

$$a = \frac{\sigma C_n}{4F \sin^2 \phi + \sigma C_n} \quad (14)$$

$$b = \frac{\sigma C_t}{4F \sin \phi \cos \phi - \sigma C_t} \quad (15)$$

and the thrust coefficient is defined as

$$C_T = 4aF(1-a). \quad (16)$$

2.2 Spera's Correction

When the axial induction factor, a , becomes larger than the critical axial induction factor a_c , the original BEM theory becomes invalid. Empirical relations between the thrust coefficient C_T and axial induction factor, a , are given by (Spera, 1994)

$$C_T = \begin{cases} 4aF(1-a) & \text{if } a \leq a_c \\ 4F(a_c^2 + a(1-2a_c)) & \text{if } a > a_c \end{cases} \quad (17)$$

Furthermore, the axial induction factor is defined as

$$a = 1 + 0.5K(1-2a_c) - 0.5\sqrt{(K(1-2a_c)+2)^2 + 4(Ka_c^2 - 1)} \quad (18)$$

with

$$K = \frac{4F \sin^2 \phi}{\sigma C_n} \quad .$$

The chord length distribution is defined as

$$c(r) = \frac{2\pi V_0 BEP}{BC_l \Omega} \quad (19)$$

with the blade element parameter

$$BEP = \frac{4a \sin \phi}{1+b} \quad .$$

3 Proposed Solution of Axial Induction Factor

The power coefficient for each blade element can be calculated by

$$C_p = \frac{dP_{out}}{dP_{win}} = \frac{dP}{dP_{win}} = \frac{4\pi r^3 \rho V_0 \Omega^2 (1-a)bFdr}{\rho \pi V_0^3 r dr} = \frac{4(r\Omega)^2 (1-a)bF}{V_0^2} \quad (20)$$

with the output power P_{out} .

The power in the wind is defined as

$$P_{win} = \frac{1}{2} \rho A V_0^3 = \frac{1}{2} \rho \pi r^2 V_0^3 \quad .$$

The maximum power coefficient is obtained by

$$\frac{dC_p}{da} = (1-a)b \frac{dF}{da} + (1-a)F \frac{db}{da} - bF = 0 \quad (21)$$

The last equation gives

$$(1-a)b \frac{dF}{da} + (1-a)F \frac{db}{da} - bF = 0 \quad (22)$$

In case $F = 1$ along the blade except for the tip, equation (22) can be written as

$$(1-a)\frac{db}{da} - b = 0. \quad (23)$$

In addition to equation (14), (Lanzafame and Messina, 2010) introduced a new relationship between axial and angular induction factors given as

$$b = \frac{1}{2}\left(\sqrt{1+ka(1-a)} - 1\right) \quad (24)$$

with

$$k = \left(\frac{2V_0}{\Omega r}\right)^2.$$

By inserting equation (24) in equation (23), the equation of axial induction factor can be obtained as follows

$$k(4a^2 - 5a + 1) + 2\left(\sqrt{1+ka(1-a)} - 1\right) = 0. \quad (25)$$

At the blade tip, where F is lower than unity, the inflow angle is less than 10° and a linearization is permissible

$$\tan \phi \approx \sin \phi \approx \phi = \frac{1-a}{\lambda_r(1+b)}$$

with λ_r is the local tip speed ratio defined as follows

$$\lambda_r = \lambda \frac{r}{R}.$$

Then, the tip loss factor can be written as

$$F_{tip} = \frac{2}{\pi} \cos^{-1}\left(\exp\left(-\frac{B(R-r)}{2r \sin \phi}\right)\right) = \frac{2}{\pi} \cos^{-1}\left(\exp\left(-\frac{B\lambda_r(R-r)(1+b)}{2r(1-a)}\right)\right). \quad (26)$$

Furthermore, the extreme value can be calculated using

$$\frac{dF}{da} = \frac{dF_{tip}}{da} = -\frac{p}{2\pi} \frac{1}{\sqrt{1-\left(\exp\frac{p(1+b)}{1-a}\right)^2}} \frac{k(1-a) + 2\left(1 + \sqrt{1+ka(1-a)}\right)}{(1-a)^2 \sqrt{1+ka(1-a)}} \exp\left(\frac{p(1+b)}{1-a}\right)$$

with

$$p = -\frac{B\lambda_r(R-r)}{2r}$$

and

$$\frac{db}{da} = \frac{k(1-2a)}{4\sqrt{1+ka(1-a)}}.$$

Using F_{tip} , dF/da and db/da , the equation (22) finally becomes

$$\begin{aligned} & \frac{-pb(1-a)(k(1-a)+4(1+b))}{2\pi(1-a)^2(1+2b)} \exp\left(\frac{p(1+b)}{1-a}\right) + \frac{k(1-a)(1-2a)}{2\pi(2b+1)} \cos^{-1}\left(\exp\left(\frac{p(1+b)}{1-a}\right)\right) \\ & - \frac{2b}{\pi} \cos^{-1}\left(\exp\left(\frac{p(1+b)}{1-a}\right)\right) = 0 \end{aligned} \quad (27)$$

The output power is given as follows

$$dP = \Omega dM \quad (28)$$

The expression for axial induction factor, a , was obtained numerically in MATLAB code by resolution the equations (25) and (27).

The method described above was carried out for the rotor blade design by applying the following steps:

1. Initialize a and b , typically $a = b = 0$.
2. Compute the inflow angle ϕ .
3. Compute the twist angle β .
4. Read the lift and drag coefficients (C_l and C_d) for each angle of attack from CFD calculation database.
5. Compute the normal and tangential coefficients (C_n and C_t) using equation (9).
6. Compute a and b by equations (25), (26) and (28).
7. Check the convergences of flow induction factors. If the changes exceed certain tolerance level, go to step 2. Else go to step 8.
8. Calculate the chord length, thrust load, torque, power.

In order to take into account radial flow along a rotating blade, to overcome this stall problem in the blade design, (Viterna and Corrigan, 1981) have proposed a stall model which was applied for predicting the lift and drag coefficients of a HAWT blade in the stall region.

For $\alpha_{stall} \leq \alpha \leq 90^\circ$, the lift and drag coefficients are as follows

$$\begin{aligned} C_l &= A_1 \sin 2\alpha + A_2 \frac{\cos^2 \alpha}{\sin \alpha} \\ C_d &= B_1 \sin^2 \alpha + B_2 \cos \alpha \end{aligned} \quad (29)$$

with

$$B_1 = C_{d \max} = 1.11 + 0.018AR \quad (\alpha = 90^\circ)$$

$$B_2 = \frac{C_{d \text{stall}} - C_{d \max} \sin^2 \alpha_{stall}}{\cos \alpha_{stall}}$$

$$A_1 = \frac{B_1}{2}$$

$$A_2 = \left(C_{l \text{stall}} - C_{d \max} \sin \alpha_{stall} \cos \alpha_{stall} \right) \frac{\sin \alpha_{stall}}{\cos^2 \alpha_{stall}}$$

and the aspect ratio $AR = \frac{r}{c}$.

For the angle of attack between 90° and 180° , the lift and drag coefficient in full stall regime can be simplified to

$$C_l = 2 \sin \alpha \cos \alpha$$

$$C_d = 2 \sin^2 \alpha .$$
(30)

4 Results and Discussion

The current approach is validated by comparing the results obtained from numerical code with the literature (Lanzafame and Messina, 2010). The characteristics of the used rotor wind turbine are given in Table 1.

Table 1. Parameters of wind turbine S809

Wind turbine type	Horizontal axis wind turbine (HAWT)
Profile type	S809
Rotational speed	72 rpm
Number of blades	2
Rated power	10 KW
Wind speed V_0	7.75 m.s^{-1}
Rotor radius	10.06 m
Type of blade	Varied chord and twisted blade

The optimal blade chord and twist angle distributions are presented in Figures (4) and (5) respectively.

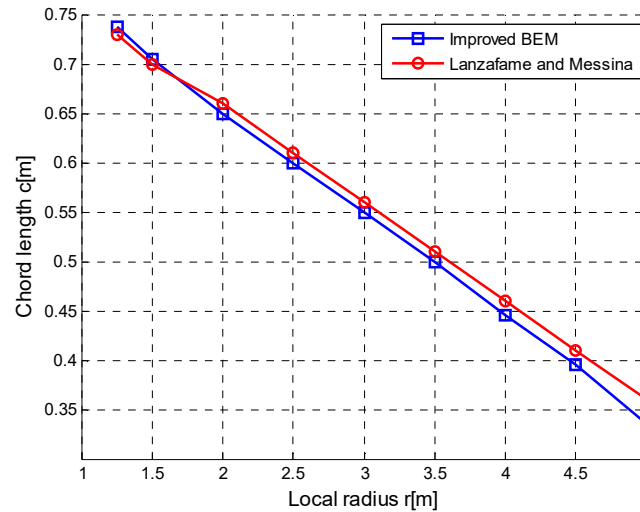


Figure 4. Chord length distribution as function of local radius

Figure 4 shows that the chord length distributions from the improved BEM analysis reaches a maximum value of 0.737 m at the root and varies nearly linearly to 0.355 m at the blade tip in good accordance to the reference. On the other hand, it can be seen that the optimized blade achieves a remarkable reduction of chord length in the region from blade root to blade tip, compared to the original rotor. At a radius of 5.03 m, the reduction of the chord length reaches a maximum value about 6.94%.

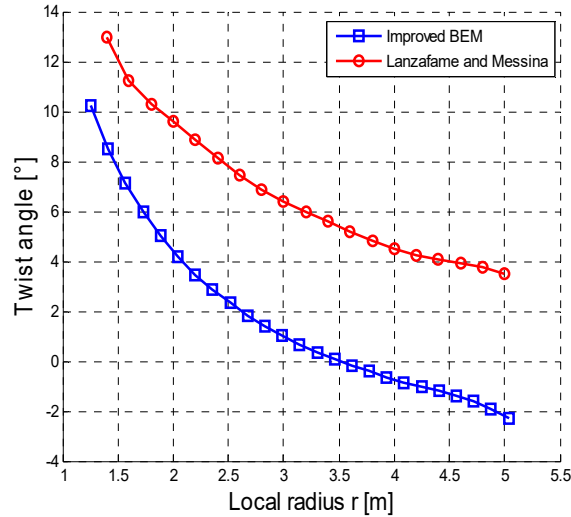


Figure 5. Twist angle distribution as a function of local radius

In order to obtain an optimal twist distribution, the optimal angle of attack of the aerodynamic profile S809 and the tip speed ratio are used because they are both critical parameters that define the profile of the blade. The addition of twisting to a wind turbine, which decreases from the root to the blade tip, is essential in order to optimize the angle of attack along the entire length of the blade for maximum power. In addition to optimizing the angle of attack, the blade is strongly twisted at the root to increase the torque generated at the root. Figure 5 shows the optimal twisting distribution that has been determined for the designed blade. The twist angle varies along the blade, from 10.25° in the root to approximately to -1.8° near the blade tip. Furthermore, a small difference between the results obtained from the numerical code compared to those presented in the literature (Lanzafame and Messina, 2010) can be seen. The twist angle is slightly smaller than the original distribution and reaches its maximum value at the blade tip.

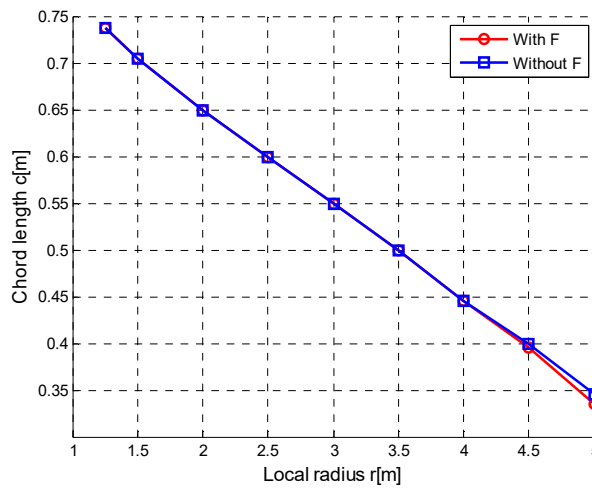


Figure 6. Chord length distribution versus local radius with and without F

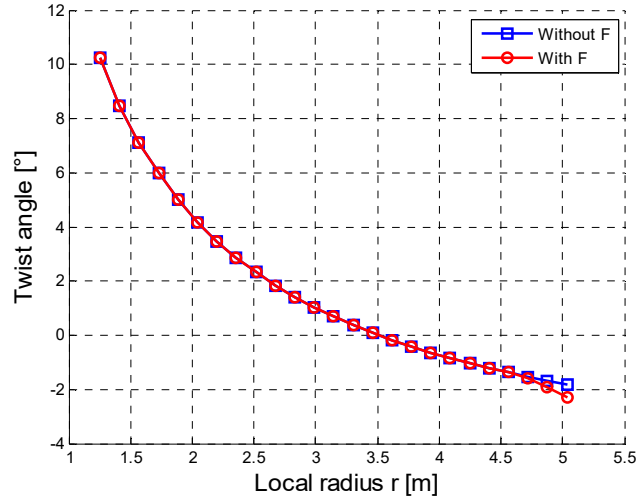


Figure 7. Twist angle distribution versus local radius with and without F

The optimal blade chord and twist angle distributions with and without the tip-hub loss factor are presented in Figures (6) and (7). The results show that the tip-hub loss factor (F) has apparent effects on both the chord and twist angle at the tip position. Differences of chord and twist angle distribution occur in the range from $0.95R$ to $1R$ tip positions when F was included. The chord reduced to 0.335 m when F was considered. However, the chord and twist angle distributions of the main part of the blade (from $0.15R$ to $0.9R$) with F are almost the same as those without F . These results led to the conclusion that the tip-hub loss factor brings visible effect on both blade chord and twist angles at the hub and tip sections.

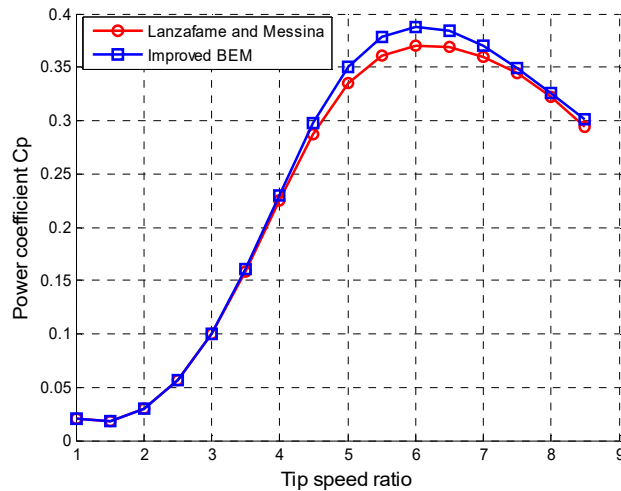


Figure 8. Power coefficient distribution versus tip speed ratio

In Figure 8, the power coefficient increases in a parabolic curve up to a maximum value of $C_p = 0.388$ which corresponds to $\lambda = 6$, after this value the power coefficient decreases. The improved BEM show a good correlation with literature (Lanzafame and Messina, 2010) ($C_p=0.375$ at $\lambda = 6$).

5 Conclusion

In the present work, the blade of the NREL phase VI wind turbine was optimized. The BEM theory used for flow analysis and the method described by Viterna and Corrigan was used for predicting the aerodynamic lift and drag coefficients of airfoils in the post-stall regime. The numerical results were compared with the available literature data showing the capability of the current numerical method in predicting the flow physics. This method gives good results compared to the CFD method and less computation time is required. The optimized blade offers a superior aerodynamic design, and presents a higher power coefficient output.

References

- Hassanzadeh, A.; Naughton, J.W.; Kelly, C.L. and Maniaci, D.C.: Wind turbine blade design for subscale testing. *Journal of physics: conferences series*, 753, (2016), 22-48.
- El khchine, Y. and Sriti, M.: Boundary layer and amplified grid effects on aerodynamic performances of horizontal axis wind turbine (HAWT). *Journal of Engineering Science and Technology*, 12 (11), (2017),3011-3022.
- Glauert, H.: *Airplane propellers*. Durrand, W.F(Ed.) Aerodynamic Theory, Springer 4, (1935),169-269.
- Manwell, J. and McGowan, J.: *Wind energy explained: theory, design and application*. second edition. John Wiley & Sons Inc, (2010),83-138.
- Singh, R. K.; Ahmed, M. R.; Zullah, M. A. and Lee, Y. H.: Design of a low Reynolds number airfoil for small horizontal axis wind turbines. *Renewable Energy*, 42, (2012), 66-76
- Maalawi, K. Y.: A practical approach for selecting optimum wind rotors. *Renewable Energy*, 28 (5), (2003), 803-822.
- Vitale, A.J.: Computational method for the design of wind turbine blades. *International Journal of Hydrogen Energy*, 33 (13), (2008), 3466-3470.
- Benini, E.: Optimal design of horizontal-axis wind turbines using blade element theory and evolutionary computation. *Journal of Solar Energy Engineering-Transactions of the ASME*, 124 (4), (2002), 357-363
- Joukowski, N.E.: Vortex theory of a rowing screw. Tr. Otd. Fiz. Nauk. Obshchestva Lubitelei Estestvozn. 16 (1) (1912)
- Wilson, R.E.; Lissaman, P.B.: *Applied Aerodynamics of Wind Power Machine*. Oregon State University, Corvallis, USA (1974)
- Vries, O.: Fluid Dynamic Aspects of Wind Energy Conversion”, Advisory Group for Aerospace Research and Development, Neuilly-Sur-Seine, France (1979)
- Sharpe, D.J.: A general momentum theory applied to an energy-extracting actuator disc. *Wind Energy*, 7 (3), (2004), 177-188.
- Sørensen, J.N.; Van Kuik, G.A.M.: General momentum theory for wind turbines at low tip speed ratios. *Wind Energy*, 14 (7), (2011), 821-839.
- Schepers, J.G.: Boorsma, K.: Final Report of IEA Task 29, Mexnext (Phase 1): *Analysis of MEXICO Wind Tunnel Measurements*. ECN Report: ECN-E-12-004 (2012)
- Lanzafame, R. and Messina, M.: Horizontal axis wind turbine working at maximum power coefficient continuously. *Renewable Energy*, 35, (2010), 301–306
- Lanzafame, R. and Messina, M.: BEM theory: How to take into account the radial flow inside of a 1-D numerical code. *Renewable Energy*, 39, (2012), 440-446
- Kim, B.; Kim, W.; Lee, S.; Bae, S. and Lee, Y.: Development and verification of a performance based optimal design software for wind turbine blades. *Renewable Energy*, 54, (2013), 166-172
- Prandtl, L. and Betz, A.: *Vier Abhandlungen zur Hydrodynamik und Aerodynamik*. Göttinger Nachr, Göttingen, 88–92 (1927)
- Spera, D.A.: *Wind Turbine Technology*. ASME Press, New York (1994)

Viterna, L.A. and Corrigan, R.D.: Fixed Pitch Rotor Performance of Large Horizontal Axis Wind Turbines.
DOE/NASA Workshop on Large Horizontal Axis Wind Turbine, Cleveland, Ohio, USA: 69–85 (1981)

Address: Younes El khchine, Engineering Sciences Laboratory, Polydisciplinary Faculty of Taza, Sidi Mohamed Ben Abdellah University, BP 1223 Road of Oujda, Taza, Morocco.
email: younes.elkhchine@usmba.ac.ma

Mohammed Sriti, Engineering Sciences Laboratory, Polydisciplinary Faculty of Taza, Sidi Mohamed Ben Abdellah University, BP 1223 Road of Oujda, Taza, Morocco.
Email: mohammed.sriti@usmba.ac.ma